WEP Warwick Evans Publishing

International Journal of Computer Science and Information Technology

ISSN: 3005-9682 (Print), ISSN: 3005-7140 (Online) | Volume 1, Number 1, Year 2023
DOI: https://doi.org/10.62051/ijcsit.v1n1.21
Journal homepage: https://wepub.org/index.php/IJCSIT/index

Research on measurement method of drilling fluid rheological parameters based on helical pipe

Jiahui Zhao[1,a], Zhongzhi Hu[1,*], Kuanliang Zhu[2,b], Yan Zhou[2,c], Wei Song[2,d]

[1] College of Mechanical Engineering, Sichuan University of Science and Engineering, Yibin, Sichuan 644002, China

[2] Jidong Oilfield Company, PetroChina Co., Ltd., Tangshan, Hebei 063000, China

*Corresponding Author: Zhongzhi Hu (Email: 1661103472@qq.com), [a] zhongzhi-hu@suse.edu.cn, [b] zkl@petrochina.com.cn, [c] jdzc_zhouyan@petrochina.com.cn, [d] jd_sw@petrochina.com.cn

ABSTRACT

Monitoring drilling fluid rheological parameters can provide a basis for assessing downhole complexities and analyzing well control risks. Among various methods for measuring drilling fluid rheological parameters, the pipe flow method allows for real-time online measurements. However, it faces limitations due to the long length of pipes and challenges in miniaturization. Based on a survey of domestic and international research, this study conducted numerical simulations to analyze the differences in flow pressure drop of drilling fluid between helical pipes and straight pipes. It clarified the impact of helical pipe structural parameters, drilling fluid process parameters, and rheological parameters on drilling fluid flow pressure drop. Utilizing the constitutive equations of Bingham, power-law, and Herschel-Bulkley fluids, a regression model was established to convert the flow pressure drop of drilling fluid between helical pipes and straight pipes. The reliability of the numerical simulation results was verified using a self-developed drilling fluid flow pressure measurement device, which yielded an average relative error of only 2.13%. These research findings provide a theoretical basis for the development of drilling fluid rheological parameter monitoring devices based on helical pipes and the corresponding software.

KEYWORDS

Drilling fluid; Rheological parameters; Pipe flow method; On-line monitoring; Spiral tube.

1. INTRODUCTION

Real-time monitoring of drilling fluid rheological parameters is crucial for enabling timely decision-making by personnel in downhole situations [1]. Among the various methods for monitoring these parameters, the pipe flow method stands out due to its high automation, resistance to blockages, and ease of achieving real-time monitoring.

However, to obtain accurate and reliable pressure differential data using the pipe flow method, measurements must be taken during the full development stage of drilling fluid in laminar flow within the pipe. This requirement results in limitations, including large equipment size, high costs, and difficulties in disassembly and transportation.

Scholars both domestically and internationally have conducted extensive research on real-time monitoring of drilling fluid rheological parameters. Zhang et al. [2, 3] analyzed the impact of parameters such as pipe diameter, drum diameter, inlet velocity, fluid density, fluid consistency index, and power-law index on the pressure drop of power-law fluids in helical pipes. Sercan Gul et al. [4-6], using experimental results and considering friction factor ratios and Dean numbers, established a

novel model for yield power-law fluids through curve fitting. Kamran Valizadeh et al. [7] employed simulation and developed a nonlinear relationship between Reynolds numbers and friction factors under different flow velocities, showing that the fluid flow remains constant within the fully developed region of the helical pipe at certain Reynolds numbers. Khaled Al-Azani et al. [8-11] utilized artificial neural networks to create predictive models that determine drilling fluid rheological properties based on mud weight, Marsh funnel viscosity, and solid content. To enhance monitoring efficiency and downsize monitoring equipment, a key strategy is to reduce the length of the piping. Substituting helical pipes for traditional straight pipes is a viable option. However, pressure differentials obtained through helical pipe measurements cannot be directly used for calculating drilling fluid rheological parameters. They require processing to be transformed into equivalents for straight pipe structures. Furthermore, previous studies have primarily focused on one type of fluid flow and neglected the diversity of non-Newtonian fluid flow. Different helical structures can also induce variations in pressure differentials within helical pipes.

In order to accurately assess the crucial factors contributing to differences in fluid pressure between helical and horizontal straight pipes and improve the reliability of helical viscometers in drilling engineering, this study conducted an analysis of the structural parameters of the pipeline, drilling fluid processes, and rheological parameters affecting drilling fluid flow pressure. A regression calculation model for helical pressure differentials was established, and experimental validation confirmed the reliability of numerical simulation results.

2. THEORY

2.1. Governing equation

Drilling fluid, being an incompressible fluid, is governed by the differential form of the mass conservation equation [12].

$$\frac{\partial \rho}{\partial t} + div(\rho u) = 0 \tag{1}$$

For incompressible fluids, the momentum conservation equation [13] (Navier-Stokes equation) can be simplified to

$$\rho \frac{\partial u}{\partial t} + \rho \frac{\partial u u_i}{\partial x_i} = f - gradp + \mu \nabla^2 u \tag{2}$$

Where: ρ is the density of the internal fluid, kg/m3; t it is the time of fluid flow in the pipe, s; u is the velocity of fluid movement, m/s; ui is the velocity component, m/s; f is the mass force of the fluid, N; p is the pressure inside the fluid, Pa; μ is the dynamic viscosity of the fluid, Pa·s.

When fluid flows within a helical pipe, it experiences the influence of centrifugal and frictional forces, resulting in an outward pressure gradient inside the pipe and the generation of secondary flow. This secondary flow affects the fluid's flow characteristics, such as increasing resistance and decreasing heat transfer efficiency. For swirling flow and changing flow direction, FLUENT provides a variety of turbulence models. Among them, the RNG k-ε model, by modifying turbulence viscosity, accounts for the effects of rotation and swirling flow within the flow [14, 15]. In this study, we employ the RNG k-ε model for numerical simulation calculations of fluid flow within helical pipes.

k Equation:

$$\frac{\partial(\rho k)}{\partial t} + \frac{\partial(\rho k u_i)}{\partial x_i} = \frac{\partial}{\partial x_j}\left[\alpha_k \mu_{eff} \frac{\partial k}{\partial x_j}\right] + G_k + \rho\varepsilon \tag{3}$$

ε Equation:

$$\frac{\partial(\rho k)}{\partial t}+\frac{\partial(\rho k u_i)}{\partial x_i}=\frac{\partial}{\partial x_j}\left[\alpha_\varepsilon \mu_{eff}\frac{\partial \varepsilon}{\partial x_j}\right]+\frac{C_{1\varepsilon}\varepsilon}{k}G_k-C_{2\varepsilon}\rho\frac{\varepsilon^2}{k} \tag{4}$$

2.2. Pressure loss in circular pipe flow

2.2.1. Along-Path and Local Resistance

Within a pipeline, the pressure loss when a viscous fluid is in motion is a combination of frictional losses along the straight sections of the pipe due to frictional resistance and local losses resulting from changes in channel geometry, flow velocity disturbances, and alterations in flow direction. The head loss along the path for the fluid can be expressed as

$$h_w=\sum h_f+\sum h_j \tag{5}$$

Where: hw is the total head loss along the fluid inside the pipe, hf is the head loss along the pipe, and hj is the local head loss.

The resistance generated by the viscous friction at the pipe wall is termed as frictional resistance along the path. The pressure drop or head loss caused by this frictional resistance is referred to as frictional pressure drop or frictional resistance loss along the path. The relationship between these two and their connection with the frictional resistance coefficient can be expressed as

$$\begin{cases}\Delta p_f=\rho g h_f=\lambda\dfrac{L}{D}\dfrac{\rho\mu_m^2}{2}\\ h_f=\lambda\dfrac{L}{D}\dfrac{u_m^2}{2g}\end{cases} \tag{6}$$

Resistance resulting from abrupt changes in flow cross-sections or alterations in flow direction is referred to as local resistance. The pressure difference or head loss caused by this local resistance is termed local pressure drop or local resistance loss. The relationship between these two variables and their connection with the local resistance coefficient can be expressed as

$$\begin{cases}\Delta p_f'=\rho g h_f'=\zeta\dfrac{\rho u_m^2}{2}\\ h_f'=\zeta\dfrac{u_m^2}{2g}\end{cases} \tag{7}$$

Where: L is the length of the pipe, m; D is the diameter of the pipe, m; um is the average velocity of the pipe cross-section; ζ is the local resistance coefficient; Δpf' is the pressure head loss; hf' is the local resistance loss.

2.2.2. Frictional resistance coefficient

The frictional resistance coefficient for laminar flow of fluid in a straight pipe is

$$\begin{cases}\lambda=\dfrac{64}{Re}\\ Re=\dfrac{\rho v d}{\mu}\end{cases} \tag{8}$$

Where: λ is the coefficient of frictional resistance in straight pipe laminar flow; Re is the Reynolds number of fluid flow in the pipe; ρ is the fluid density, kg/m³; v is the fluid flow velocity, m/s; d is the diameter of the pipe, m; μ is the fluid dynamic viscosity, mpa·s.

The frictional resistance coefficients for helical pipes and curved pipes are given by equations (9) and (10), respectively[17].

Laminar flow:

$$\frac{\lambda_c}{\lambda_s} = 1 + 0.033\left(lgDe_m\right)^{4.0} \quad \left(1 < De_m < 3000\right) \tag{9}$$

Turbulent flow:

$$\lambda_c = \lambda_s + 0.03\left(d/2R_c^{'}\right)^{0.5} \quad \left(4500 < Re < 10^5\right) \tag{10}$$

Where: λc is friction resistance coefficient of bending pipe; λs is the straight pipe friction resistance coefficient, λs =64/Re (laminar flow), λs =0.3164/R0.25 (turbulent flow);

where:

$$\begin{cases} R_c^{'} = R_c\left[1 + \left(h/2\pi R_c\right)^2\right] \\ De_m = Re\sqrt{d/2R_c^{'}} \end{cases} \tag{11}$$

Experimental results [18] indicate that the transitional Reynolds number for the transition from laminar to turbulent flow in helical pipes can be expressed as:

$$Re_c = 20000\left(d/2R_c^{'}\right)^{0.32} \tag{12}$$

Where: Rc' is the modified radius of curvature of the Helical pipe, Dem is called the modified Dean number, Rc is the radius of curvature of the Helical pipe, m; d is the diameter of the Helical pipe, m; h is the pitch of the Helical pipe, m.

3. NUMERICAL SIMULATION SCHEME AND MODELING

3.1. Numerical simulation scheme

To analyze the differences in monitoring drilling fluid rheological parameters between helical and straight pipes, establish a rheological parameter calculation model, clarify the impact of pipeline structural parameters and drilling fluid rheological parameters on fluid flow pressure drop, we conducted a sensitivity analysis on the parameters shown in Table 1, providing their respective benchmark values.

Table 1. Benchmark values of parameters

variable name	Initial value	symbol
Pipe diameter	20 mm	r
Pitch of Helical pipe	287 mm	P
Helical pipe bottom diameter round	630 mm	D
Inlet flow velocity	0.5 m/s	v
Density	2.2×10^3 kg/m³	ρ
Fluidity index	0.5	n
Consistency coefficient	0.7	K
Yield stress	1.0 pa	τ

Then the fluid initially enters the pipe, its velocity is not fully developed. There is a velocity development region during which pressure measurements cannot be taken. To ensure the reliability of pressure measurement data, monitoring surfaces for internal pressure values are established every 100 mm within the fully developed velocity region. As shown in Figure 1, the average of pressure differences (Δp1, Δp2.....Δpi) taken at intervals of 100 mm along the pipe is used as the pressure drop (Δp) in this paper. A similar monitoring approach is implemented for the helical pipe in its stable central velocity region.

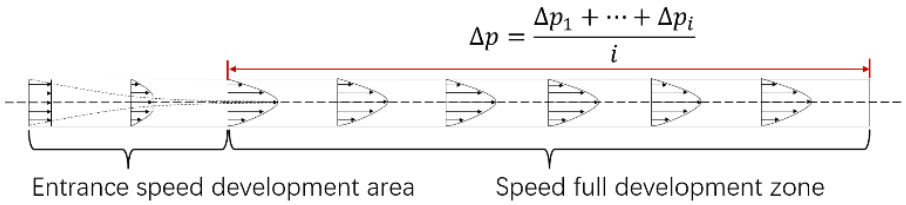

Fig.1 Flow velocity distribution diagram in pipe

3.2. Meshing and independence verification

When fluid flows, it creates a viscous layer near the wall, within which significant changes occur in velocity distribution, pressure distribution, and shear stress distribution. Hence, grid refinement is essential in the boundary layer region. As shown in Figure 2, the average pressure of drilling fluid flow in the fully developed velocity region is calculated for minimum grid sizes of 1, 2, 3, 4, 5, and 6 mm.

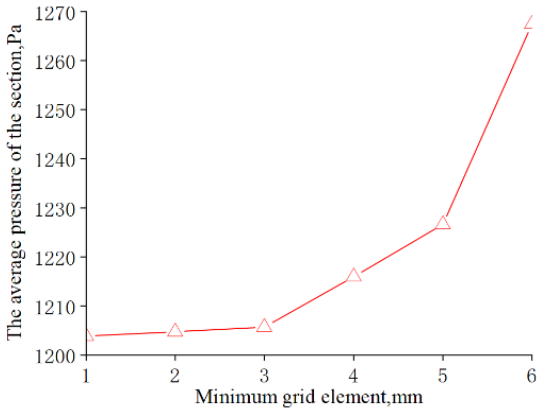

Fig.2 Grid independence verification results

From Figure 2, it is evident that as the minimum grid size remains below 3 mm, the sensitivity of the calculations to the number of grids gradually levels off, and the pressure stabilizes. The grid partition is illustrated in Figure 3.

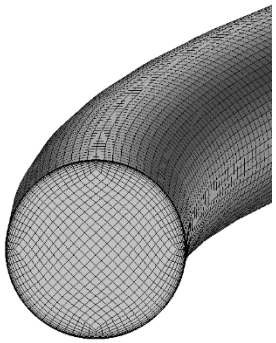

Fig.3 Local grid diagram of helical pipe

4. RESULTS ANALYSIS

4.1. Structural parameters of the pipe

4.1.1. Pipe diameter

The pipe diameters are set to 15, 16, 17, 18, 19, and 20 mm, and Figure 4 presents the numerical simulation results of drilling fluid flow pressure drop under varying diameter conditions.

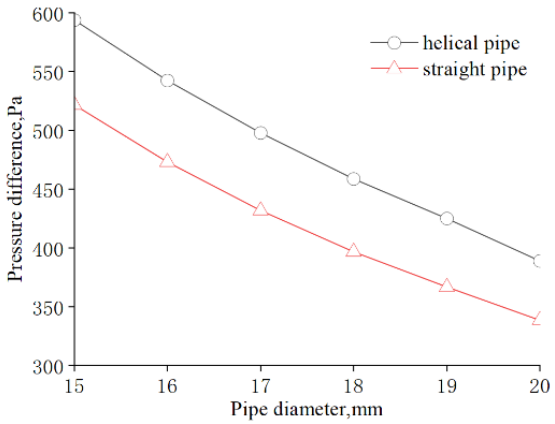

Fig.4 Effect of pipe diameter on flow pressure difference of drilling fluid

From Figure 4, it can be observed that the drilling fluid flow pressure drop in both curved and straight pipes follows a similar trend as the diameter changes. It approximately linearly decreases with increasing diameter, and the pressure drop in the helical pipe is higher than that in the straight pipe.

4.1.2. Pitch of helical pipe

A large pitch in the helical pipe is not conducive to minimizing the space occupied by the measurement pipeline. Therefore, the analyzed pitch values for the helical pipe are 20 mm, 40 mm, 60 mm, 80 mm, 100 mm, and 120 mm. The results are shown in Figure 5.

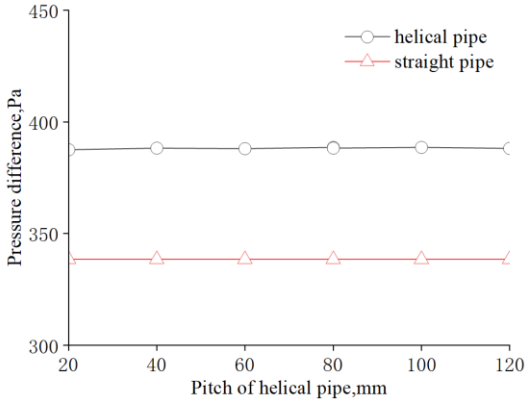

Fig.5 Effect of Helical pipe pitch on drilling fluid flow pressure difference

From Figure 5, it can be observed that as the pitch of the helical pipe increases, the flow pressure drop of the drilling fluid inside the pipe remains largely unchanged. The reason for the flow pressure drop in the helical pipe is due to frictional losses along the pipeline and changes in flow direction. When the pitch of the helical pipe changes, the curvature of the helical pipe itself remains constant, meaning there is no alteration in the flow direction of the drilling fluid inside the pipe.

4.1.3. Helical pipe base diameter circle diameter

The bottom diameters of the helical pipe are taken as 230 mm, 430 mm, 630 mm, 830 mm, 1030 mm, and 1230 mm, as illustrated in Figure 6 with the numerical simulation results.

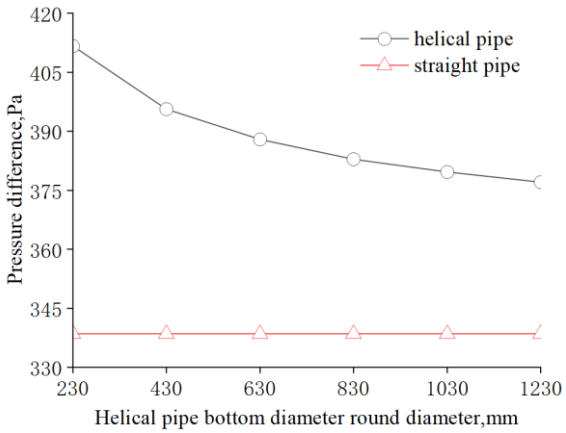

Fig.6 Effect of Helical pipe bottom diameter on flow pressure difference of drilling fluid

From Figure 6, it can be observed that the drilling fluid pressure drop inside the pipe decreases with the increase in the bottom diameter of the helical pipe. The primary reason for this is that when fluid flows within the helical pipe, it experiences the centrifugal force. As the bottom diameter of the cylindrical helical structure increases, the reduced curvature results in a decrease in centrifugal force within the helical pipe. This leads to a reduction in the local pressure loss of drilling fluid as it flows inside the pipeline.

4.2. Process and performance parameters of drilling fluid

4.2.1. Inlet flow velocity

Entrance velocities were set to 0.5 m/s, 0.6 m/s, 0.7 m/s, 0.8 m/s, 0.9 m/s, and 1 m/s, respectively. The pressure drop inside the straight pipe and helical pipe with respect to entrance velocity is illustrated in Figure 7.

The bottom diameters of the helical pipe are taken as 230 mm, 430 mm, 630 mm, 830 mm, 1030 mm, and 1230 mm, as illustrated in Figure 6 with the numerical simulation results.

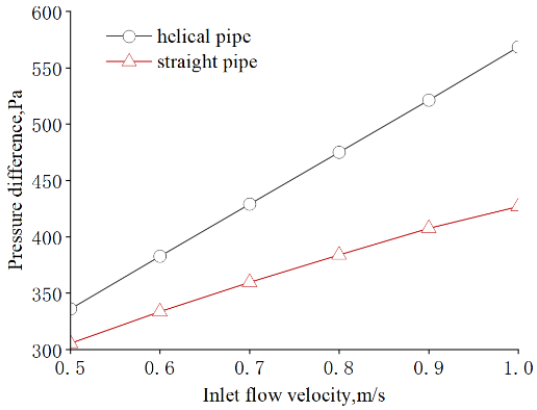

Fig.7 Effect of Helical pipe bottom diameter on flow pressure difference of drilling fluid

Figure 7 reveals that the drilling fluid flow pressure drop in both the helical pipe and the horizontal straight pipe increases as the inlet velocity rises. Furthermore, the pressure drop in the helical pipe exhibits a greater rate of increase compared to the straight pipe. In contrast to the straight pipe, when fluid flows inside the helical pipe, there is an additional local pressure loss resulting from changes in flow direction, which also increases with the flow velocity.

4.2.2. Density

The drilling fluid density was varied at values of 1000 kg/m³, 1200 kg/m³, 1400 kg/m³, 1600 kg/m³, 1800 kg/m³, and 2000 kg/m³. The numerical simulation results are depicted in Figure 8.

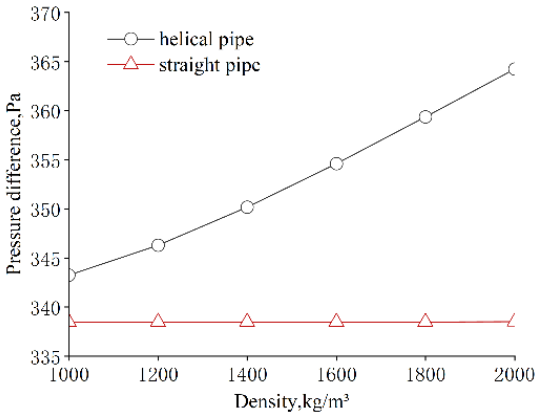

Fig.8 Effect of density on flow pressure difference of drilling fluid

Figure 8 demonstrates that as the drilling fluid density increases, the pressure drop within the helical pipe continually grows, while the pressure drop within the straight pipe remains largely constant. This is attributed to the fact that when the drilling fluid density increases, its inertia force also increases, leading to a greater local pressure loss caused by changes in flow direction. In contrast, in the laminar flow within the straight pipe, the fluid velocity remains steady, kinetic energy remains unchanged, and the flow pressure drop stays relatively constant.

4.2.3. Fluidity index n

The flow behavior index was varied at values of 0.4, 0.45, 0.5, 0.55, 0.6, 0.65, and 0.7. The numerical simulation results are presented in Figure 9.

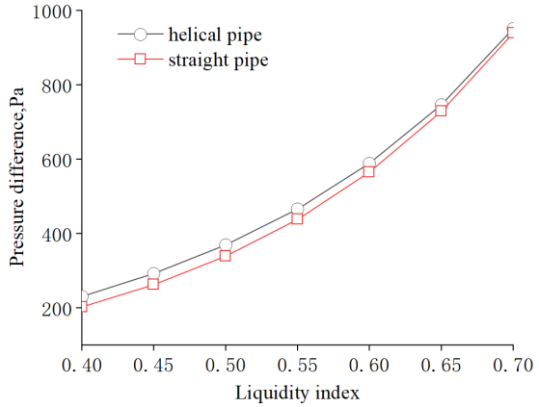

Fig.9 Effect of fluidity index on flow pressure difference of drilling fluid

From Figure 9, it is evident that the flow pressure drop of drilling fluid increases with the rise in the consistency index. The pressure drop values in the helical pipe closely resemble those in the straight pipe, and their trends align. As the consistency index of the drilling fluid increases, its apparent viscosity also increases. This leads to a greater shear stress required for fluid flow and subsequently results in larger pressure losses.

4.2.4. Consistency coefficient K

The viscosity coefficient values of 0.5, 0.6, 0.7, 0.8, 0.9, and 1 were respectively selected, and the numerical simulation results are shown in Figure 10.

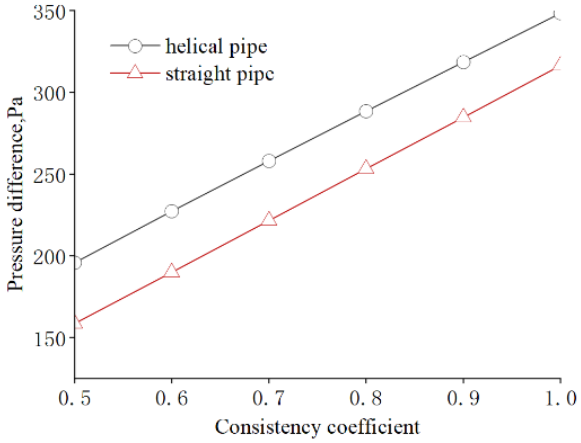

Fig.10 Effect of consistency coefficient on flow pressure difference of drilling fluid

From Figure 10, it can be observed that the pressure drop of drilling fluid increases with the rise in the consistency coefficient. Moreover, the extent of pressure increase within the helical pipe aligns with that of the straight pipe. This is because, as the consistency coefficient increases, the viscosity of the drilling fluid also increases. This implies that the drilling fluid encounters greater resistance during its flow, consequently leading to an increase in pressure drop.

4.2.5. Yield stress

The yield stresses are taken as 1 Pa, 5 Pa, 10 Pa, 15 Pa, 20 Pa, and 25 Pa, respectively, and the numerical simulation results are shown in Fig. 11.

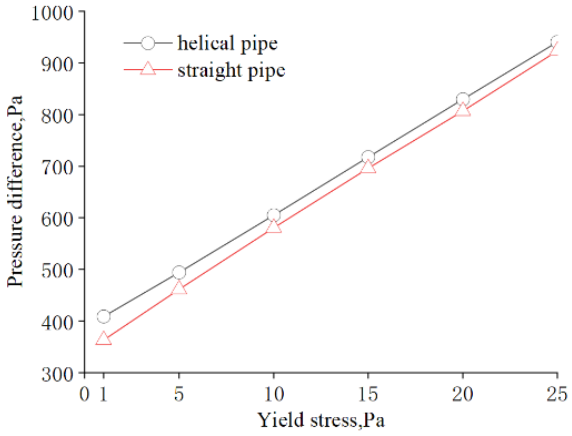

Fig.11 Effect of yield stress on flow pressure difference of drilling fluid

From Figure 11, it is evident that the flow pressure drop of drilling fluid increases progressively with the rise in yield stress. Moreover, the extent of pressure increase within the helical pipe aligns with that of the straight pipe. An increase in the yield stress of drilling fluid implies that the fluid needs to withstand greater shear stress to overcome its yield stress for flow, leading to an increase in pressure drop within the pipeline.

Based on the above analysis, it can be concluded that the impact of helical pipe pitch on drilling fluid flow pressure drop can be neglected, while other parameters have varying degrees of influence. Numerical simulation results for the remaining parameters were fitted, resulting in seven fitting formulas as shown in Table 2. In these formulas, "y" represents the ratio of pressure drop between the straight and helical pipes. From Table 2, it can be seen that the relationships between the influencing factors and the pressure drop ratio between the two pipe types are nonlinear, with all correlation coefficients exceeding 0.99.

Table 2. Fitting result

Influence factor	Fitting formula	Correlation index
Inlet flow velocity	$y = 0.705e^{-0.822v} + 0.441$	1.00
Density	$y = -0.079e^{\rho/2507.91} + 1.104$	1.00
Consistency Coefficient	$y = -0.401e^{-1.588k} + 0.99$	1.00
Liquidity index	$y = -0.584e^{-n/0.746} + 1.219$	1.00
Yield stress	$y = 0.8893 \cdot \tau^{0.0311}$	1.00
Pipe diameter	$y = 14.222e^{-d/2.262} + 0.86$	1.00
Helical pipe base Diameter round	$y = -0.142e^{-D/409.21} + 0.904$	1.00

5. ESTABLISHMENT OF REGRESSION MODELS FOR CONVERTING PRESSURE DROP BETWEEN HELICAL AND STRAIGHT PIPES

To obtain an accurate computational model that describes the pressure drop in helical pipes, we conducted numerical simulations for both helical and straight pipes. Based on these results and considering the parameters involved in the commonly used rheological models for drilling fluid, namely, the Bingham, power-law, and Herschel-Bulkley models, we established a regression model for converting pressure drops between helical and straight pipes. This model serves as a foundation for calculating drilling fluid rheological parameters.

5.1. Bingham fluid

The constitutive equation for the Bingham fluid model is given by

$$\tau_0 = \tau + \eta \cdot \gamma \tag{13}$$

where τ0 is the shear stress, Pa; γ is the shear rate, s-1.

The main factors related to the flow pressure drop of Bingham fluid are flow velocity, density, yield stress, helical pipe diameter, and bottom circular diameter. Performing multivariate nonlinear regression analysis on these five influencing factors yields.

$$\begin{aligned} \Delta p_s = (&-1.93e^{-5}dD + 0.0084\rho + 2.964e^{-7}\rho D - 4.34e^{-5}\rho d + 4.94e^{-6}\rho\tau - 3.31e^{-5}v\rho \\ &- 0.133v^2 - 7.13e^{-8}\rho^2 - 0.000272\tau^2 + 0.0031d^2 - 1.37e^{-7}\rho^2)\Delta p_c \end{aligned} \tag{14}$$

Where: Δps is the differential pressure of the horizontal straight pipe, Pa; Δpc is the differential pressure of the helical pipe, Pa.

The variance analysis of the regression equation results shows an R2 value of 0.997, indicating that the pressure drop of Bingham fluid in both the helical and straight pipes can be reliably converted using Equation (14).

5.2. Power-law fluid

The constitutive equation for the Power-Law fluid model is given by

$$\tau_0 = k\gamma^n \tag{15}$$

The main factors related to the flow pressure drop of the Power-Law fluid are flow velocity, density, flow behavior index, consistency coefficient, helical pipe diameter, and bottom circle diameter. Performing multivariate nonlinear regression analysis on these six influencing factors yields:

$$\Delta p_s = (-4.95e^{-5}dD + 6.74e^{-4}\rho + 6.1e^{-7}\rho D - 5.643e^{-5}\rho d - 2.65e^{-4}\rho n + 0.0003\rho k - 8.9e^{-5}v\rho - 0.059v^2 - 4.564e^{-8}\rho^2 - 0.32k^2 + 0.92n^2 + 0.005d^2 - 1.997e^{-7}D^2)\Delta p_c \quad (16)$$

Where: n is the fluidity index, dimensionless; k is the consistency factor, dimensionless.

The variance analysis of the regression equation shows an R2 value of 0.987, indicating that the pressure drop of the Power-Law fluid in both helical and straight pipes can be reliably converted using Equation (16).

5.3. Herschel-Bulkley fluid

The constitutive equation for the Herschel-Bulkley fluid model is given by pattern is

$$\tau_0 = \tau + k\gamma^n \quad (17)$$

The main factors associated with the flow pressure drop of the Herschel-Bulkley fluid are flow velocity, density, flow behavior index, consistency coefficient, yield stress, helical pipe diameter, and bottom circular diameter. Conducting a multivariate nonlinear regression analysis on these seven influencing factors yields the following results:

$$\Delta p_s = (-4.853e^{-5}dD + 6.74e^{-4}\rho + 6.006e^{-7}\rho D - 5.62e^{-5}\rho d + 3.99e^{-6}\rho\tau - 2.74e^{4}\rho n + 3.017e^{-4}\rho k - 8.663e^{-5}v\rho - 0.0625v^2 - 4.626e^{-8}\rho^2 - 0.321k^2 + 0.934n^2 - 2.1e^{-4}\tau^2 + 0.0045d^2 - 1.982e^{-7}D^2)\Delta p_c \quad (18)$$

The variance analysis of the regression equation shows an R2 value of 0.978, indicating that the pressure drop of the Herschel-Bulkley fluid in both helical and straight pipes can be reliably converted using Equation (18).

6. EXPERIMENTAL VERIFICATION

To validate the reliability of the numerical simulation results, experimental tests on the flow pressure drop in straight pipes were conducted using an existing and custom-built drilling fluid flow pressure loss test experimental apparatus. This apparatus comprises a pump, flowmeter, pressure sensors, PVC pipes, sample barrel and a supporting frame. The experimental apparatus's structure is depicted in Figure 12.

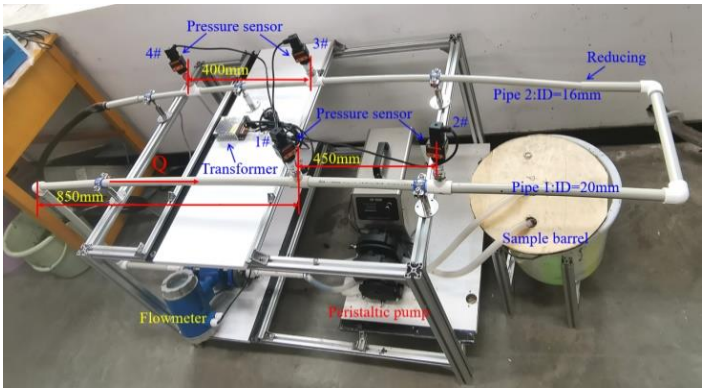

Fig.12 Experimental apparatus

First, we tested the pressure drop of clear water in the pipeline. Then, we calculated the pressure drop of clear water under laminar flow conditions using theoretical formulas. We compared the calculated pressure drop with the experimentally measured pressure drop to validate the reliability of the experimental setup. Eight flow rate settings were established, and the pressure drop of clear water was calculated using the theoretical formula. The calculated pressure drop was compared to the values shown in Figure 13.

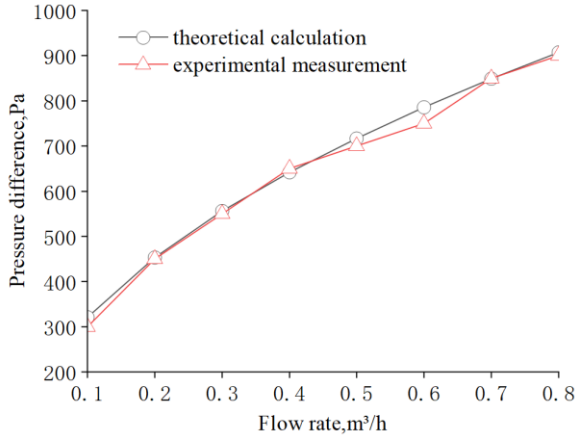

Fig.13 Comparison of theoretical calculation and measurement results

From Figure 13, it can be observed that the theoretical pressure drop calculations for the straight pipe segment closely align with the experimental results for pure water. The calculated average deviation is 12.38 Pa, with an average relative error of 2.2%. This demonstrates the capability of the experimental apparatus to accurately measure pressure drops in straight pipe sections.

For the drilling fluid from a well in the Chongqing shale gas block, the flow pressure drop was compared to numerical simulation results. The drilling fluid had a density of 2.963 g/cm3 and exhibited power-law behavior with rheometer measurements yielding values of 206 (φ600), 129 (φ300), 98.5 (φ200), 61 (φ100), 18 (φ6), and 16 (φ3) for apparent viscosities. This behavior corresponds to a power-law model with calculated parameters of n = 0.67 and k = 1.02. Figure 14 illustrates the comparison between experimental and numerical results for flow pressure drop in pipes with inner diameters of 20 mm and 16 mm.

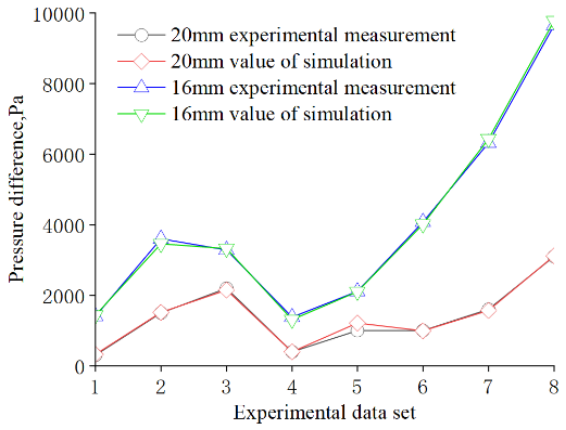

Fig.14 Comparison of numerical simulation and experimental measurement results

From Figure 14, it is evident that the experimental results closely match the simulation results, with an average relative error of 2.13% for pressure drop. This experimental validation indirectly confirms the reliability of the numerical simulation results.

7. CONCLUSION

(1) The study investigated the influence of structural parameters of the helical pipe, process parameters, and rheological parameters of drilling fluid on the pressure drop of drilling fluid inside the pipe. Among the structural parameters of the pipeline, the flow pressure drop of drilling fluid in the helical pipe decreases as the helical pipe diameter and the bottom circular diameter increase. The effect of the helix pitch on the pressure drop can be neglected. Therefore, when establishing the

pressure drop conversion model between the helical pipe and the straight pipe, it is only necessary to modify the diameter and bottom circular diameter of the helical pipe.

(2) Among the process parameters of drilling fluid, the flow pressure drop of drilling fluid inside the helical pipe increases with the increase in velocity, density, flow behavior index, consistency coefficient, and yield stress. Density does not affect the flow pressure drop inside the straight pipe, and the impact of the other parameters on the pressure drop inside the straight pipe is consistent with that in the helical pipe.

(3) Based on the numerical simulation results, a pressure drop calculation model for drilling fluid in the three rheological modes was established for the helical pipe. The correlation coefficients of each mathematical model are all above 0.97. This model can convert the flow pressure drop of drilling fluid inside the helical pipe into the pressure drop in the straight pipe, which can be used for calculating drilling fluid rheological parameters.

(4) Using the constructed straight pipe experimental platform, the pressure drop values in the straight pipe section of drilling fluid samples were measured. The analysis results showed that the maximum relative error between experimental data and simulation data was 3.9%, verifying the reliability of the straight pipe simulation data

REFERNECES

[1] WANG Peng.LIU Wei.ZHANG Guo. 2022.Current situation of automatic monitoring device for drilling fluid properties and suggestions for improvement.Drilling and Production technology[J]. 45(3):42-47.

[2] ZHANG Jiaxing.ZHANG Quansheng.YU Guijie. 2020.Analysis of influence factors of continuous tube power law fluid flow and pressure drop[J].Petroleum Machinery. 48(3):140-146.

[3] LI Yue.WANG Yahong.LI He.et al.Comparative study on pressure loss of two helical tubes with different sections[J]. 2015. General Machinery. 9:94-97.

[4] Gul S. Erge O. Oort E V. Helical Pipe Viscometer System for Automated Mud Rheology Measurements: IADC/SPE International Drilling Conference and Exhibition[C]. 2020.

[5] Gul S. Erge O. van Oort E. Frictional pressure losses of Non-Newtonian fluids in helical pipes: Applications for automated rheology measurements[J]. 2020. Journal of Natural Gas Science and Engineering. 73:103042.

[6] Shaukat A C. Pressure Drop in Archimedian Helical Tubes [J]. Industrial & Engineering Chemistry Research. 1971.

[7] Karimi Vajargah A. van Oort E. Determination of drilling fluid rheology under downhole conditions by using real-time distributed pressure data[J]. 2015. Journal of Natural Gas Science and Engineering. 24:400-411.

[8] Gomaa I. Elkatatny S. Abdulraheem A. Real-time determination of rheological properties of high over-balanced drilling fluid used for drilling ultra-deep gas wells using artificial neural network[J]. 2020. Journal of Natural Gas Science and Engineering. 77:103224.

[9] Gowida A. Elkatatny S. Abdelgawad K. et al. Newly Developed Correlations to Predict the Rheological Parameters of High-Bentonite Drilling Fluid Using Neural Networks[J]. 2020. Sensors. 20(10):2787.

[10] Al-Azani K E S A A. Real Time Prediction of the Rheological Properties of Oil-Based Drilling Fluids Using Artificial Neural Networks[J]. 2018. SPE Kingdom of Saudi Arabia Annual Technical Symposium and Exhibition.

[11] Rooki R. Estimation of Pressure Loss of Herschel-Bulkley Drilling Fluids During Horizontal Annulus Using Artificial Neural Network[J]. 2015. Journal of dispersion science and technology. 36(2):161-169.

[12] Zhou Y S S N. New Friction Factor Correlations of Non-Newtonian Fluid Flow in Coiled Tubing[J]. 2006. SPE Drilling & Completion. 21(1):68-76.

[13] Bowman A J P H. CFD Study on Laminar Flow Pressure Drop and Heat Transfer Characteristics in Toroidal and Helical Coil System[J]. 2004. International Mechanical Engineering Congress and Exposition.

[14] Galván S R M G F. Assessment Study of K-ε Turbulence Models and Near-Wall Modeling for Steady State Swirling Flow Analysis in Draft Tube Using Fluent[J]. 2011. Engineering Applications of Computational Fluid Mechanics. 5(4):459-478.

[15] Rahimzadeh H M R S H. Simulating Flow Over Circular Spillways by Using Different Turbulence Models[J]. 2012. Engineering Applications of Computational Fluid Mechanics. 6(1):100-109.

[16] REN Anlu, LIN Jianzhong, RUAN Xiaodong. Hydrome chanics [M]. 2013. Beijing: Tsinghua University press.

[17] HUANG Weixing. Analysis and calculation of fluid flow problems[M]. 2022. Beijing: Chemical Industry Press.

[18] Ali S Z A H. Head Loss and Critical Reynolds Numbers for Flow in Ascending Equiangular Helical Tube Coils[J]. 1979. Industrial & Engineering Chemistry Process Design and Development.2(18):349-353.

DECLARATIONS

Ethical Approval

This study did not involve human or animal subjects, and thus, no ethical approval was required. The study protocol adhered to the guidelines established by the journal.